IEICE TRANSACTIONS

on Fundamentals of Electronics, Communications and Computer Sciences

DOI:10.1587/transfun.2024EAL2071

Publicized:2024/11/28

This advance publication article will be replaced by the finalized version after proofreading.

A PUBLICATION OF THE ENGINEERING SCIENCES SOCIETY

The Institute of Electronics, Information and Communication Engineers

Kikai-Shinko-Kaikan Bldg., 5-8, Shibakoen 3 chome, Minato-ku, TOKYO, 105-0011 JAPAN

LETTER

A Low-Cost Angle Super-Resolution FMCW Phased Array Radar based on TSPW for Automotive Applications

Duo Zhang[†a)], ***Nonmember and*** **Shishan Qi**[††], ***Nonmember***

SUMMARY A low-cost super-resolution frequency modulated continuous wave (FMCW) phased array radar employing a single radio-frequency (RF) channel sampling scheme is proposed. Since the conventional phased array radar lacks element-level array signals, it cannot achieve angle super-resolution. By exploiting time sequence phase weighting (TSPW) technology, the proposed radar can obtain the element-level array signals without connecting additional transmit/receive (T/R) components to each antenna element, as that in element-level digital arrays. Furthermore, the freedom of the array has been further enhanced by exploiting the nested array structure. Numerical simulation results are presented to demonstrate the effectiveness of the proposed system.

key words: *time sequence phase weighting(TSPW), single RF channel, nested array, FMCW radar*

1. Introduction

In recent years, millimeter-wave frequency modulated continuous wave (FMCW) radars have been widely used in automotive applications, such as advanced driver-assistance systems [1-4], active cruise control [5-7], and automatic parking [8-10]. By performing a two-dimensional (2-D) Fast Fourier Transform (FFT), the range and speed information of multiple targets can be simultaneously obtained from the frequency spectrum. To obtain the angular information at a relatively low cost, a conventional scheme is to use passive phased array antennas with electronic beam scanning or monopulse angle measurement methods. However, the angular resolution of this array is limited by the Rayleigh criterion. It cannot effectively distinguish between targets whose angular separation is less than 3 dB beamwidth.

To address this issue, a typical approach is to use Digital Beamforming (DBF) or Multiple-Input Multiple-Output (MIMO) technology, which performs simultaneous multichannel sampling on the whole antenna array. This kind of array is also known as an element-level digital array [11]. By integrating an independent RF signal sampling channel behind each antenna element, the spatial signals received by each antenna element can be preserved. Then, by employing spatial spectrum estimation algorithms, such as multiple signal classification (MUSIC) [12] or estimation of signal parameters via rotational invariance techniques (ESPRIT) [13], super-resolution angle estimation can be achieved. However, since the signal sampling channel is one of the most expensive components of a radar system [14-16] and this technology requires multiple signal sampling channels, the overall cost and complexity are significantly higher than the phased arrays.

To solve this problem, many efforts have been proposed to reduce the number of sampling channels in the past. In [17, 18], a time division multiplexing single channel receiver scheme called spatial multiplexing of local elements was proposed. Based on the structure, [19, 20] proposed a low-cost 24GHz FMCW radar. In [21], a randomized switched antenna FMCW radar system was proposed, where the receiving antennas are randomly switched to a single receiving channel. [22] proposed a low-cost time-modulated wideband antenna array. [23] proposed a single channel RF method based on Code Division Multiple Access (CDMA) technology to reduce the size and cost. Similarly, [24] proposed a time sequenced phase weighting (TSPW) technique that only needs a single RF channel. The original element-level signal of the array can be recovered by dispreading processing. The impact of imperfections in $0/\pi$ phase shifter network of TSPW was studied in [25]. [26] applied the compressed-sensing theory to TSPW array to reduce the sampling rate.

To increase the degrees of freedom (DOF) of linear arrays, [27] proposed a nested array geometry. By processing multi-channel sampling signals, this array can obtain a DOF far greater than that of the original array. [28, 29] proposed an improved array geometry to reduce the mutual coupling. However, since this technology also requires element-level array signals, it is unsuitable for conventional phased arrays.

In this letter, a low-cost super-resolution FMCW radar combined with TSPW technology and nested geometry is proposed. With a single RF channel only, the proposed array can obtain the element-level signals received by each antenna element. Additionally, taking advantage of the nested array geometry, the DOF of the proposed array is significantly higher than that of the conventional element-level digital array and TSPW array with the same number of physical array elements.

†The author is with the Nanjing Institute of Technology, 211167 Nanjing, China
††The author is with the School of Electronic Engineering and Optoelectronic Technology, Nanjing University of Science and Technology, Xiao Ling Wei 200#, 210094 Nanjing, China
a) E-mail:duozhang@njit.edu.cn

2. Scheme of the Nested-TSPW array radar

The structure of the Nested-TSPW array radar is shown in Fig. 1. It uses a wide-beam transmission antenna as the radiating element. The main beam width is sufficiently broad to cover the road ahead, thereby eliminating the need for mechanical or electronic scanning to obtain adequate echo gain during operation. The receive antenna is a two-level nested array that contains two uniform linear arrays (ULA), namely the inner array and the outer array. The number of array elements of the inner and the outer array are denoted as N_1 and N_2, respectively. The total number of antenna elements is N=N_1+N_2. The space between adjacent elements is denoted as d_{L1} and d_{L2}, which satisfy

$$d_{L2} = (N_1 + 1)d_{L1} \tag{1}$$

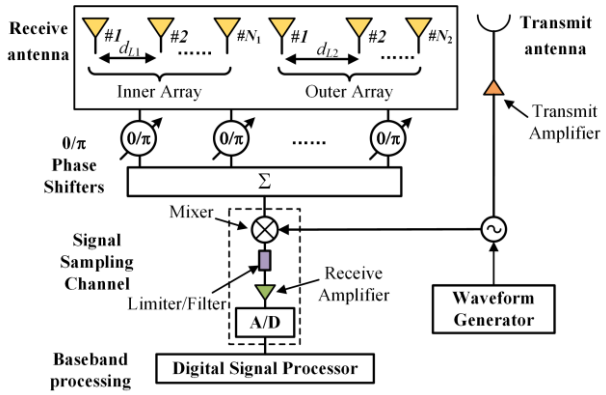

Fig. 1 The structure of the Nested-TSPW array radar.

According to Fig. 1, each array sensor of the receive antenna is connected to a 0/π phase shifter. The weighted array signals are combined at RF domain. The 0/π phase shifter only provides 0 or π phase shift value and can be controlled by the digital signal processor (DSP). After down-conversion and filtering, the single channel weighted signals are digitized and sampled by the analog-to-digital converter (ADC).

3. Signal model and processing algorithm

3.1 Signal model

The transmitting signal is FMCW signal, which can be described in the time domain with multicycle sweep as

$$s_s(t) = \exp[j2\pi(f_0(t+mT) + \frac{1}{2}\alpha t^2)] \ , \ 0 \le t \le T \tag{2}$$

where f_0 is the starting frequency, T is the sweep repetition period, t indexes the fast time snapshot, m = 0, 1, ⋯, M-1 is the number of slow time snapshot, α=B/T is the chirp rate, and B is the bandwidth. Let R_k, V_k, θ_k denote the initial range, relative radial velocity, and azimuth angle of the kth target, respectively. The signals received by different antenna elements have a relative phase difference $\Delta\varphi_{k,n}$ associated with the direction of arrival (DOA). It can be written as $\Delta\varphi_{k,n}$=$j2\pi d_n \sin\theta_k/\lambda$, where λ is the wavelength of the carrier frequency, d_n is the distance of the nth antenna element with respect to the reference element. For the proposed system, d_{L1} = $\lambda/2$ and d_{L2} = $(N_1+1)\lambda/2$. The antenna element positions are denoted as $\mathbf{D}$=$\{nd_{L1}, n=1, \cdots, N_1\} \cup \{nd_{L2}, n=1, \cdots, N_2\}$. The echo of the kth target received by nth antenna is

$$s_{r,k,n}(t) = \exp\left\{ j2\pi\left[f_0\left(t + mT - \tau_k\right) + \frac{1}{2}\alpha(t-\tau_k)^2 \right] + \Delta\phi_{k,n} \right\} \tag{3}$$

where τ_k=$2[R_k$+$V_k(t$+$mT)]/c$ is the time delay associated with the kth target and c denotes the electromagnetic wave propagation speed. Assuming there are K targets in front of the radar, the final signals recevied by the nth antenna is $S_n(t)$= $\sum_{k=0}^{K-1} s_{r,k,n}(t)$ +$z(t)$, where $z(t)$ is the zero-mean additive white Gaussian noise (AWGN).

The sampling process and the radar data cube are illustrated in Fig. 2. The echo signals are weighted by the

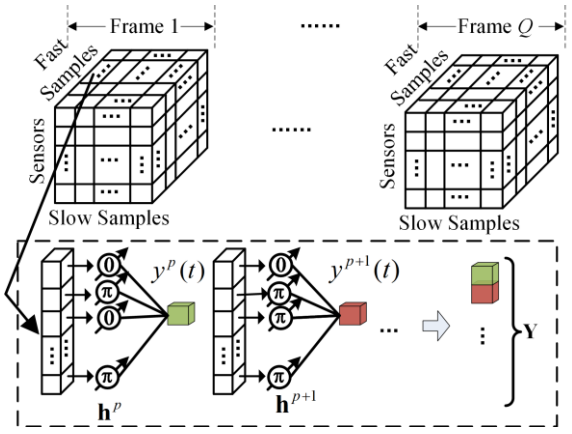

Fig. 2 The radar data cube and weighting combination process.

0/π phase shifters. For an array with N elements, these shifters change state N times during one single-channel sampling cycle to form a Walsh-Hadamard matrix $\mathbf{H}$. The 0 and π weighting states correspond to the values 1 and -1 in $\mathbf{H}$, respectively. The weighting values of the pth sample can be considered as a vector $\mathbf{h}^p$=$[h_0^p, h_1^p, \cdots, h_{N-1}^p]$, where $0 \le p \le N-1$. After combining, a single-channel signal is obtained, which can be represented as

$$y(t_p) = \sum_{n=0}^{N-1} h_n^p S_n(t_p) = \mathbf{h}^p \mathbf{S}(t_p) \tag{4}$$

where $\mathbf{S}(t_p)$=$[S_0(t_p), S_1(t_p), \cdots, S_{N-1}(t_p)]^T$.

After mixing and passing through a low-pass filter, a zero intermediate frequency (IF) single-channel signal is obtained, which is denoted as

$$y_{IF}(t_p) = \sum_{n=0}^{N-1} h_n^p S_n^{IF}(t_p) = \mathbf{h}^p \mathbf{S}_{IF}(t_p) \tag{5}$$

where

$$S_n^{IF}(t_p) = \sum_{k=0}^{K-1} \exp[j4\pi(\frac{R_k\alpha}{c}t_p + \frac{V_k f_0}{c}mT + \frac{\pi R_k f_0}{c}) - \Delta\phi_{k,n}] \tag{6}$$

, $\mathbf{S}_{IF}(t_p)$=$[S_0^{IF}(t_p), S_1^{IF}(t_p), \cdots, S_{N-1}^{IF}(t_p)]^T$. A single-channel

sampling cycle contains N zero-IF signals. Thus, the samplings obtained within a sampling period is

$$\mathbf{Y}=\begin{bmatrix} y_{IF}(t_0) \\ \vdots \\ y_{IF}(t_{N-1}) \end{bmatrix}=\begin{bmatrix} \mathbf{h}^0\mathbf{S}_{IF}(t_0) \\ \vdots \\ \mathbf{h}^{N-1}\mathbf{S}_{IF}(t_{N-1}) \end{bmatrix} \tag{7}$$

According to Eqs. (5) and (6), it can be seen that the effective information of the target is contained in $S_n^{IF}(t_p)$. For an element-level digital array, the signal $S_n^{IF}(t_p)$ is considered to be the original element-level array signals, which can be directly acquired and processed for angle super-resolution algorithms. However, for a single-channel array, the only signal that can be obtained is $y_{IF}(t_p)$. It cannot be directly used for angle super-resolution.

3.2 Signal processing

The signal processing flowchart of the proposed system is illustrated in Fig. 3. For angle super-resolution, the original element-level array signals should be obtained first. According to Eq. (5), the zero-IF signal of one target is a sinusoidal signal. When viewed from a multi-period perspective, it is a frequency-modulated signal. Since the phase of the single-channel signal is time-varying during a single-channel sampling period, directly applying the TSPW technology to the samplings $\mathbf{Y}$ to recover the original array signals will result in significant errors, thereby degrading the performance of the angle super-resolution algorithm. Therefore, a pre-reconstruction process is added before applying the TSPW technology to recover the original signal.

The essence of the errors when directly recovering the signal is that the time-varying signal, with different weighting states, has been sampled at different times. The signals with the same weighting value are missing. Considering the maximum detection range to be R_{max}, let the minimum sampling frequency of the fast snapshot for the proposed radar system F_s satisfies

$$F_s \geq 2Nf_{b,\max} \tag{8}$$

where $f_{b,\max}$ is the maximum frequency of the zero-IF signals, corresponding to R_{max}. The switch frequency of the 0/π phase shifters is equal to F_s. Then, the proposed system satisfies the Nyquist-Shannon sampling theorem and the algorithm based on shannon interpolation proposed in [30] can be used to obtain the missing signals. Denote the pre-restored signals of one sampling cycle as $\widehat{\mathbf{G}}$. It is an $N\times N$ matrix and can be written as

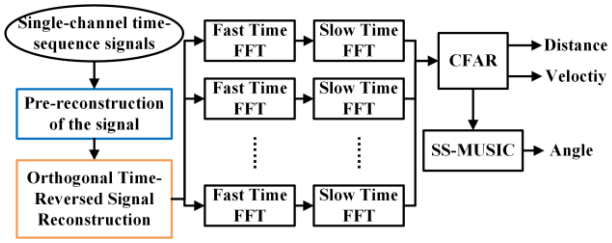

Fig. 3 Signal processing flowchart.

$$\mathbf{G}=\begin{bmatrix} \boldsymbol{h}^0\mathbf{S}_{IF}(t_0) & \boldsymbol{h}^0\mathbf{S}_{IF}(t_1) & \cdots & \boldsymbol{h}^0\mathbf{S}_{IF}(t_{N-1}) \\ \boldsymbol{h}^1\mathbf{S}_{IF}(t_0) & \boldsymbol{h}^1\mathbf{S}_{IF}(t_1) & \cdots & \boldsymbol{h}^1\mathbf{S}_{IF}(t_{N-1}) \\ \vdots & \vdots & \ddots & \vdots \\ \boldsymbol{h}^{N-1}\mathbf{S}_{IF}(t_0) & \boldsymbol{h}^{N-1}\mathbf{S}_{IF}(t_1) & \cdots & \boldsymbol{h}^{N-1}\mathbf{S}_{IF}(t_{N-1}) \end{bmatrix} \tag{9}$$

where $\widehat{\mathbf{S}_{IF}(t_p)}$ is the recovered missing signals under the same weighting value. Then, Eq. (9) can be rewritten in matrix form as

$$\mathbf{G}=[\mathbf{HS}'(t_0)\quad \mathbf{HS}'(t_1)\quad \cdots\quad \mathbf{HS}'(t_{N-1})] \tag{10}$$

The Walsh-Hadamard matrix has the property that $\mathbf{H}^T\mathbf{H}=N\mathbf{I}_N$ and $\mathbf{H}^{-1}=1/N\mathbf{H}^T$. By exploiting the property, the reconstructed element-level array signal can be expressed as

$$\mathbf{S}=\mathbf{H}^{-1}\mathbf{G}=\frac{1}{N}\mathbf{H}^T\mathbf{G}=[\mathbf{S}'(t_0)\ \cdots\mathbf{S}'(t_p)\cdots\ \mathbf{S}'(t_{N-1})] \tag{11}$$

The signal $\mathbf{S}'(t_p)$ contains the same information about the targets as that contained in $\mathbf{S}_{IF}(t_p)$. One slow sampling period contains multiple $\tilde{\mathbf{S}}$. Multiple slow sampling data form a frame of data. The frequency of the signal is

$$f_b=2R_k\alpha/c=\frac{2R_k\alpha}{c} \tag{12}$$

Additionally, the phase changes over different sweep periods, which are associated with the Doppler frequency f_d caused by the relative motion of the targets. The Doppler frequency is

$$f_d=2V_k f_0/c=\frac{2V_k f}{c} \tag{13}$$

In practice, by applying 2-D FFT, the range-Doppler frequency spectrum is obtained. The constant false alarm rate (CFAR) detector is applied to detect the target. The range and velocity of the kth target are

$$R_k=\frac{f_bTc}{2B},\ V_k=\frac{f_dc}{2f_0} \tag{14}$$

Once the targets have been detected, the angle estimation can be performed. Since the reconstructed signal has the element-level information, the angular super-resolution algorithm can be applied. Assuming a peak, detected from the recovered signals of the nth elements, is located at the αth row and βth column in the range-Doppler frequency spectrum. Denote the peak data of the qth frame of the nth element as $x_{\alpha,\beta}^n(q)$. The snapshot for DOA is

$$\mathbf{x}_{\alpha,\beta}(q)=[x_{\alpha,\beta}^0(q),\cdots,x_{\alpha,\beta}^{N-1}(q)]^T \tag{15}$$

The covariance matrix $\mathbf{R}$, after the accumulation of Q frames, can be estimated as

$$\mathbf{R}=\frac{1}{Q}\sum_{q=1}^{Q}\mathbf{x}_{\alpha,\beta}(q)(\mathbf{x}_{\alpha,\beta}(q))^H \tag{16}$$

The signal of the difference co-array (DCA) is

$$\mathbf{X}=vec(\mathbf{R}) \tag{17}$$

where $vec(\mathbf{R})$ is the vectorization of the matrix $\mathbf{R}$. By employing the spatial smoothing multiple signal classification (SS-MUSIC) algorithm [27], angle super-resolution can be achieved.

4. Simulation results

The simulation parameters for the proposed system are detailed in Table 1. A wide beam antenna with a 3dB beamwidth of 40° is used as the transmission antenna. The beamwidth is sufficient to cover the road area 200 meters ahead of the radar, and beam scanning is not required during operation. The element locations of the recevied array is $[0.5\lambda, 1\lambda, 1.5\lambda, 2\lambda, 2.5\lambda, 5\lambda, 7.5\lambda, 10\lambda]$ with N_1=N_2=4.

Table I Parameters for simulations

Parameter	Value
Initial Sweep Frequency	24.125 GHz
Sweep Bandwidth	200 MHz
Sweep Repetition Period	0.2 ms
Signal Wavelength	12.4 mm
Switch Frequency of Phase Shifter	25 MHz
Number of Frames	16
Number of Antennas	8
ADC Sampling Rate	50 MHz
Number of frames	16

Consider 4 targets located in front of the system with initial distances and velocities R_1=100 m, R_2=70 m, R_3=40 m, R_4=90 m, V_1=0 m/s, V_2=3 m/s, V_3=5 m/s, and V_4=9 m/s. The angles are −60°, −30°, 25°, and 50°. The signal-noise ratio (SNR) is set to -5dB. The commonly used range-velocity spectrum and the DOA estimation outcomes produced by the proposed radar are shown in Fig. 4. Then, the snapshot $\mathbf{x}_{\alpha,\beta}(q)$, corresponding to these target is obtained. It can be seen that the range, velocity, and angle information of the targets are estimated correctly by the proposed radar system.

Next, we investigate the angular super-resolution ability of the proposed system. A conventional phased array

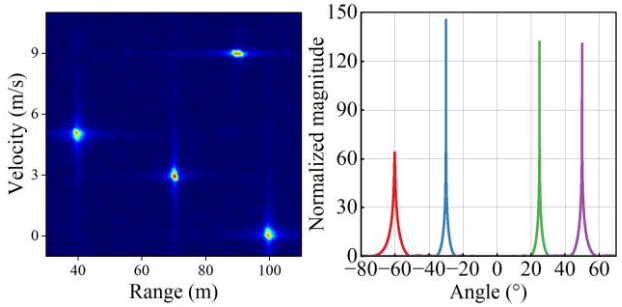

Fig. 4 Performances of the proposed system. (a) Range-velocity spectrum (b) DOA spectrum.

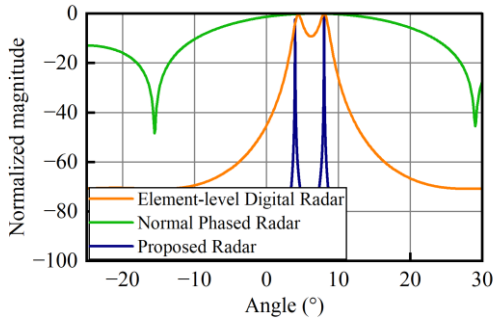

Fig. 5 The spatial spectrum of two closely spaced sources, which cannot be distinguished by the range-velocity spectrum.

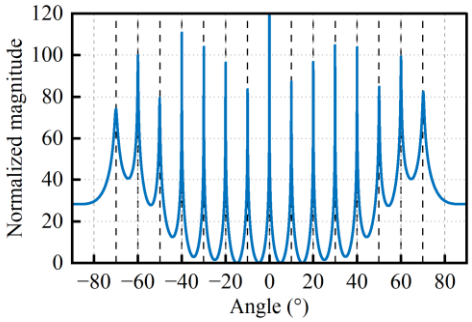

Fig. 6 The spatial spectrum when the number of targets exceeds the number of array elements.

radar and an element-level digital array radar are also presented for comparison. Both employ an 8-element ULA as the receiving antenna. The element spacing is 0.5λ. Apart from the switch frequency of phase shifter, the other system parameters are the same as those presented in Table I. According to the configuration, the angular resolution of the normal phased radar is 14.3°. Consider two targets located in front of the system with angles of arrival at 4° and 8°. The initial distances and velocities are R_1=R_2=100 m, V_1=V_2=10 m/s. The SNR is set to -5dB. In this scenario, these two targets cannot be distinguished from the range-velocity spectrum. For DOA estimating, the phased array radar exploits the classical beamscan method, element-level digital array radar uses the MUSIC algorithm, and the proposed system employs the SS-MUSIC algorithm. Fig. 5 shows the DOA estimation results for these three systems. It can be found that these two targets have been clearly distinguished by the proposed system and the digital array radar. Since the angular separation is smaller than the Rayleigh resolution criterion, the conventional phased array radar cannot correctly resolve these two targets as expected.

To demonstrate the capability of the proposed radar to resolve more sources than sensors, we set 15 targets in front of the system, whose spatial incidence angles are uniformly positioned from −70° to 70°. The normalized spatial MUSIC spectrum is shown in Fig. 6. It can be observed that our proposed radar can resolve all 15 targets correctly, while a conventional element-level digital radar fails.

5. Conclusion

In this letter, we propose a low-cost, super-resolution FMCW phased array radar via a single RF channel sampling scheme to reduce hardware cost and design complexity. The structure and the signal processing method are introduced. Simulation results demonstrate the effectiveness of the proposed system. Future work includes analyzing the reconstruction error and finding a more rapid reconstruction algorithm.

Acknowledgments

This work was funded by projects including the Scientific Research Foundation for the Highlevel Personnel of Nanjing Institute of Technology (grant: YKJ2019109).

References

[1] H. Sim, et al.: "Road environment recognition for automotive FMCW RADAR systems through convolutional neural network," IEEE Access 8 (2020) 141648 (DOI: 10.1109/ACCESS.2020.3013263).

[2] J. Zhao, et al.: "Hybrid antenna arrays with high angular resolution for 77 GHz automotive radars," IEICE Electronics Express 17 (2020) 20190687 (DOI: 10.1587/elex.16.20190687).

[3] J.-H. Choi, et al.: "Mutual interference suppression using clipping and weighted-envelope normalization for automotive FMCW radar systems," IEICE Trans. Commun. E99.B (2016) 280 (DOI: 10.1587/transcom.2015EBP3152).

[4] J. Lee, et al.: "Joint angle, velocity, and range estimation using 2D MUSIC and successive interference cancellation in FMCW MIMO radar system," IEICE Trans. Commun. E103.B (2020) 283 (DOI: 10.1587/transcom.2018EBP3330).

[5] X. Gao, et al.: "MIMO-SAR: A hierarchical high-resolution imaging algorithm for mmWave FMCW radar in autonomous driving," IEEE Trans. Veh. Technol. 70 (2021) 7322 (DOI: 10.1109/TVT.2021.3092355).

[6] D. Mao, et al.: "Angular superresolution for forward-looking scanning radar with pulse interference using cross-domain low-rank and sparse optimization," IEEE Trans. Geosci. Remote Sens. 62 (2024) 1 (DOI: 10.1109/TGRS.2024.3422271).

[7] Y.-S. Won, et al.: "24GHz FMCW radar module for pedestrian detection in crosswalks," IEICE Trans. Electron. E102.C (2019) 416 (DOI: 10.1587/transele.2018ECS6019).

[8] Y. C. Kan, et al.: "A parking monitoring system using FMCW radars," APSIPA ASC (2021) 1931 (DOI:

[9] S. Sun, et al.: "MIMO radar for advanced driver-assistance systems and autonomous driving: advantages and challenges," IEEE Signal Processing Magazine 37 (2020) 98 (DOI: 10.1109/MSP.2020.2978507).

[10] J. M. García, et al.: "MIMO-FMCW radar-based parking monitoring application with a modified convolutional neural network with spatial priors," IEEE Access 6 (2018) 41391 (DOI: 10.1109/access.2018.2857007).

[11] S. H. Talisa, et al.: "Benefits of digital phased array radars," Proc. IEEE 104 (2016) 530 (DOI: 10.1109/JPROC.2016.2515842).

[12] R. Schmidt: "Multiple emitter location and signal parameter estimation," IEEE Trans. Antennas Propag. 34 (1986) 276 (DOI: 10.1109/TAP.1986.1143830).

[13] R. Roy and T. Kailath: "ESPRIT-estimation of signal parameters via rotational invariance techniques," IEEE Trans. Acoust. Speech Signal Process. 37 (1989) 984 (DOI: 10.1109/29.32276).

[14] L. Moon-Sik, et al.: "System modeling and signal processing for a switch antenna array radar," IEEE Trans. Signal Process. 52 (2004) 1513 (DOI: 10.1109/TSP.2004.827204).

[15] Z. G. Xu, et al.: "A sparse uniform linear array DOA estimation algorithm for FMCW radar," IEEE Signal Process Lett. 30 (2023) 823 (DOI: 10.1109/lsp.2023.3292739).

[16] W. Ahmad, et al.: "Low RF-complexity digital transmit beamforming for large-scale millimeter wave MIMO systems," IEEE Trans. Wireless Commun. 21 (2022) 8308 (DOI: 10.1109/TWC.2022.3165577).

[17] J. D. Fredrick, et al.: "A smart antenna receiver array using a single RF channel and digital beamforming," IEEE Trans. Microwave Theory Tech. 50 (2002) 3052 (DOI: 10.1109/TMTT.2002.805150).

[18] J. D. Fredrick, et al.: "Smart antennas based on spatial multiplexing of local elements (SMILE) for mutual coupling reduction," IEEE Trans. Antennas Propag. 52 (2004) 106 (DOI: 10.1109/TAP.2003.818798).

[19] M. S. Lee and Y. H. Kim: "Design and performance of a 24-GHz switch-antenna array FMCW radar system for automotive applications," IEEE Trans. Veh. Technol. 59 (2010) 2290 (DOI: 10.1109/TVT.2010.2045665).

[20] M.-S. Lee: "Signal modeling and analysis of a planar phased-array FMCW radar with antenna switching," IEEE Antennas Wirel. Propag. Lett. 10 (2011) 179 (DOI: 10.1109/LAWP.2011.2123074).

[21] C. Hu, et al.: "Randomized switched antenna array FMCW radar for automotive applications," IEEE Trans. Veh. Technol. 63 (2014) 3624 (DOI: 10.1109/TVT.2014.2308895).

[22] G. Bogdan, et al.: "Time-modulated antenna array for real-time adaptation in wideband wireless systems—part I: design and dharacterization," IEEE Trans. Antennas Propag. 68 (2020) 6964 (DOI: 10.1109/TAP.2019.2902755).

[23] F. Tzeng, et al.: "A CMOS code-modulated path-sharing multi-antenna receiver front-end," IEEE J. Solid-State Circuits 44 (2009) 1321 (DOI: 10.1109/JSSC.2009.2015810).

[24] J. Zhang, et al.: "Single RF channel digital beamforming multibeam antenna array based on time sequence phase weighting," IEEE Antennas Wirel. Propag. Lett. 10 (2011) 514 (DOI: 10.1109/LAWP.2011.2157073).

[25] J. Zhang, et al.: "Comparison of correction techniques and analysis of errors for digital beamforming antenna array with single RF receiver," IEEE Trans. Antennas Propag. 60 (2012) 5157 (DOI: 10.1109/TAP.2012.2207695).

[26] D. Zhang, et al.: "Array signal recovery algorithm for a single-RF-channel DBF array," EURASIP Journal on Advances in Signal Processing 2016 (2016) 99 (DOI: 10.1186/s13634-016-0391-6).

[27] P. Pal and P. P. Vaidyanathan: "Nested arrays: a novel approach to array processing with enhanced degrees of freedom," IEEE Trans. Signal Process. 58 (2010) 4167 (DOI: 10.1109/TSP.2010.2049264).

[28] C. L. Liu and P. P. Vaidyanathan: "Super nested arrays: linear sparse arrays with reduced mutual coupling—part I: fundamentals," IEEE Trans. Signal Process. 64 (2016) 3997 (DOI: 10.1109/TSP.2016.2558159).

[29] C. L. Liu and P. P. Vaidyanathan: "Super nested arrays: linear sparse arrays with reduced mutual coupling—part II: high-order extensions," IEEE Trans. Signal Process. 64 (2016) 4203 (DOI: 10.1109/TSP.2016.2558167).

[30] D. Zhang, et al.: "A novel motion compensation method for single RF channel digital beamforming array," APMC (2015) 1 (DOI: 10.1109/APMC.2015.7413590).